

FIG. 2. Time-of-flight (TOF) neutron-diffraction pattern for cubic KCN III with the Maxwellian background mathematically removed. The solid line shows the result of simultaneously fitting all of the peaks using the variable intensity fit as described in Sec. III of the text. The fit is not extended to the (100) peak at the extreme right end of the pattern because of a frame overlap problem which caused the background to rise slightly here. The calculated position of the (100) peak is shown by a vertical arrow. The peaks due to the alumina ( $\text{Al}_2\text{O}_3$ ) pressure cell are given with their hexagonal indices.

eters which are the only adjustable parameters affecting the peak positions.  $\alpha_h$  and  $f_h$  are the peak amplitudes of the KCN peaks and the  $\text{Al}_2\text{O}_3$  peaks, respectively, and  $v$  is an overall intensity factor for  $\text{Al}_2\text{O}_3$ . The KCN peak amplitudes  $\alpha_h$  are treated as variable parameters while the relative amplitudes  $f_h$  for  $\text{Al}_2\text{O}_3$  are held fixed at values determined from a pure  $\text{Al}_2\text{O}_3$  diffraction pattern. Pb peaks, if present, are treated in the same manner as  $\text{Al}_2\text{O}_3$  peaks. This allows an accurate subtraction of  $\text{Al}_2\text{O}_3$  and Pb peaks from the pattern, particularly as these in all cases were very small at the  $60^\circ$  scattering angle. In some regions of the diffraction pattern the intensities obtained from this type of analysis are slightly in error because the assumed shape for the Maxwellian with the three variable parameters is not sufficient to exactly fit the background over the entire spectrum. For the least-squares technique described here, the ratio of  $\chi^2$  to the number of degrees of freedom which we shall designate the "goodness of fit" should lie between 0.8 and 1.2 for a perfect statistical fit. In what follows we shall refer to the fit summarized in Eq. (1) as the variable intensity fit.

Since the TOF diffraction method employs a con-

tinuous range of neutron wavelengths ( $\lambda$ ), the measured intensities are modified by the thermal neutron spectrum and by a  $\lambda^4$  multiplication.<sup>16</sup> Relative structure factors were determined from the measured intensities [ $I_h^{\text{TOF}} = \alpha_h S_i (\pi/4 \ln 2)^{1/2}$ ] according to the relation

$$m_h |F_h|^2 \propto I_h^{\text{TOF}} / \lambda^4 I_0(\lambda), \quad (2)$$

where  $m_h$  is the multiplicity for the peak with label  $h$  in the diffraction pattern,  $F_h$  is the structure amplitude including Debye-Waller factors, and  $I_0(\lambda)$  characterizes the neutron flux from the reactor. In our case  $I_0(\lambda)$  was determined from a measurement of the direct beam transmitted through the pressure cell containing the sample using a detector matched to those used for the  $30^\circ$  and  $60^\circ$  scattering angles, and so  $I_0(\lambda)$  should implicitly contain absorption and multiple scattering corrections for both the sample and pressure cell as well as detector efficiency corrections. In fits to the diffraction pattern for well-known cubic materials it was found that the measured  $I_0(\lambda)$  predicted structure factors for the diffraction peaks associated with the longer neutron wavelengths which were too low. In order to fit the measured intensities

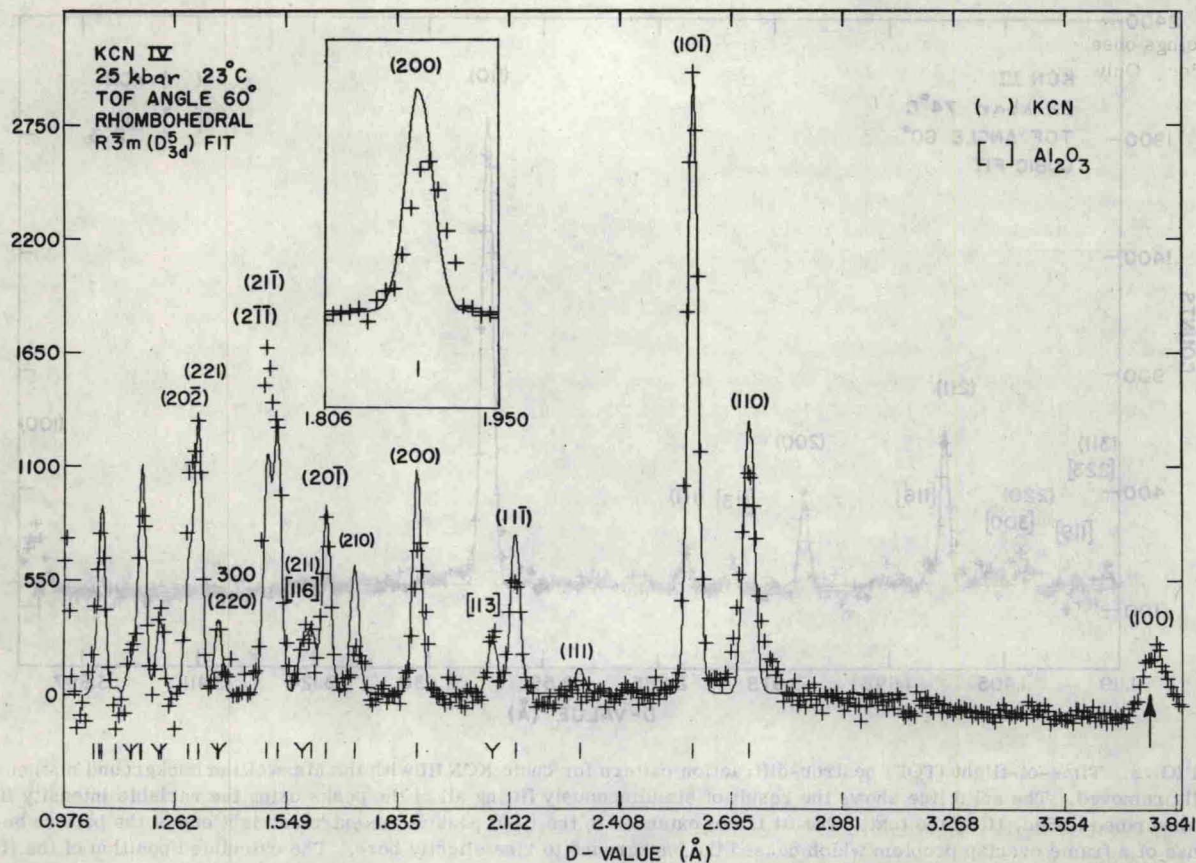


FIG. 3. TOF neutron-diffraction pattern for KCNIV. The solid line shows the result of simultaneously fitting all of the peaks assuming the space group  $R\bar{3}m(D_{3d}^5)$  with the cyanide ion lying along the primary axis of the rhombohedral unit cell. (See Sec. III of the text.) The displacement of the (100) and the (200) peaks from their exact rhombohedral positions is emphasized by the inset above the (200) peak and the vertical arrow showing the calculated position of the (100) peak. The vertical lines just below the diffraction pattern give the rhombohedral line positions while the positions of the observable  $Al_2O_3$  lines are marked by the symbol Y.

TABLE I. Plane spacing and intensity of KCNIII at 74°C and 22 kbar.

cubic $hkl$	$d_{obs}^a$ (Å)	$d_{calc}$ (Å)	$m  F_{hkl} _{obs}^2$	$m  F_{hkl} _{calc}^2$	
				$Pm\bar{3}m(O_h^1)$	Free rotation model
100	$3.807 \pm 0.002$	3.8080	$16.4 \pm 2.9$	18.6	18.6
110	$2.6912 \pm 0.0011$	2.6926	$82.1 \pm 5.6$	79.8	79.0
111	$2.1982 \pm 0.0017$	2.1985	$5.8 \pm 0.5$	5.9	3.8
200	$1.9049 \pm 0.0007$	1.9040	$14.5 \pm 1.7$	14.5	16.1
210		1.7030	<2.4	0.4	0.1
211	$1.5538 \pm 0.0016$	1.5546	$29.5 \pm 2.6$	30.9	27.0
220		1.3463	<4.8	7.6	6.0
300 221	$1.2694 \pm 0.0028$	1.2693	$5.2 \pm 3.3$	5.5	6.4
310		1.2042	<2.0	1.4	7.4
311	$1.1498 \pm 0.0016$	1.1482	$9.6 \pm 2.4$	9.7	8.8
Lattice parameter = $3.8080 \pm 0.0003$ Å			Refinement		
Unit cell volume = $55.22 \pm 0.01$ Å <sup>3</sup>			fitting parameters		
			$B_K(\text{Å}^2)$	$2.6 \pm 0.6$	2.23
			$B_{CN}(\text{Å}^2)$	$3.9 \pm 0.8$	6.21
			C-N Bond length (Å)	$1.23 \pm 0.02$	1.2
			R value for fit (%)	4.1	11.5

<sup>a</sup>No entry in column 2 signifies that it was not intense enough to determine  $d$ -spacing.